Journal of Pharmaceutical and Biomedical Analysis 54 (2011) 660–666

Contents lists available at ScienceDirect

Journal of Pharmaceutical and Biomedical Analysis

journal homepage: www.elsevier.com/locate/jpba

In-line reaction monitoring of entacapone synthesis by Raman spectroscopy and multivariate analysis

Predrag Novak[a,*], Andrea Kišić[a], Tomica Hrenar[a], Tomislav Jednačak[a], Snežana Miljanić[a], Gordana Verbanec[b]

[a] Department of Chemistry, Faculty of Natural Sciences, University of Zagreb, Horvatovac 102a, HR-10000 Zagreb, Croatia
[b] PLIVA Croatia Ltd., Prilaz baruna Filipovića 29, HR-10000 Zagreb, Croatia

ARTICLE INFO

Article history:
Received 8 June 2010
Received in revised form
10 September 2010
Accepted 18 October 2010
Available online 27 October 2010

Keywords:
Entacapone
In-line reaction monitoring
Raman spectroscopy
Multivariate analysis

ABSTRACT

In-line Raman spectroscopy and multivariate analysis were used to monitor Knoevenagel condensation reaction, the final step in preparation of drug entacapone. By applying a fiber optical Raman probe immersed into a reaction vessel Raman spectra of the reaction mixture were recorded *in situ* during the entacapone synthesis in toluene, heptane and isobutyl acetate. Due to the complexity of the measured spectra, the obtained data were analyzed and interpreted by means of principal component analysis.

It has been shown that progress of this reaction can be monitored in real-time and reaction end points can be determined in different solvents. The reaction was found to be the fastest in heptane due to the lower loss of the catalyst. For a comparison the reaction was independently monitored by *off-line* Raman spectroscopy and liquid chromatography which confirmed the results obtained *in-line*.

The results presented here have shown that this *in-line* approach can be used as a fast, non destructive and reliable method to monitor the Knoevenagel reaction in real time. The knowledge gained in this study can further be exploited for the industrial process control.

1. Introduction

In recent years, it has become obvious that for the production of drugs new challenges have to be dealt with including the control of parameters defining the quality of particles during the preparation process as well as isolation of the active substances. The use of sophisticated, advanced and efficient analytical methods and techniques is of utmost importance in modern pharmaceutical manufacturing processes [1–3]. The standard monitoring procedures usually include analytical measurements with samples taken out of the chemical reactor and hence do not provide information on chemical reactions in real time. The transport of sample may cause many dynamic processes to occur which can alter the composition of the reaction mixture and lead to significant measurement errors. Major limitations to improve the control of physical and chemical processes arise from the lack of versatile, accurate and reliable *in-line* sensors. Hence, new approaches and methodologies are needed for a better quality control and higher product efficiency. The main advantages of *in-line* methods are that they are not time-consuming and offer a non-destructive, non-invasive and real time detection of different physical and chemical transformations of the reactants and products during the laboratory and production processes. It is very important to monitor the chemical reaction in real time to ensure that it is proceeding as expected and to change the reaction conditions if deviations of the expected reaction profile occur or even to stop the reaction to prevent the waste of a batch.

Vibrational spectroscopy (IR and Raman) has been applied extensively for the characterization of pharmaceuticals. Drug crystallization process, polymorphism, production of dosage forms and chemical reactions of drugs have recently been studied by *in situ* or *in-line* FTIR and Raman spectroscopies [4–15]. The physicochemical properties of bioactive compounds such as, solubility and permeability depend on their crystallographic forms which may have a dramatic impact on the therapeutic efficacy and on the manufacturing of the final dosage forms. Hence, it is crucial to develop tools that will enable understanding and better control of both chemical reaction and crystallization process in real time. The main prerequisites for using Raman spectroscopy are that reactants and product should be Raman active and present in adequate concentrations in order to detect start and end points of chemical reactions or to obtain kinetic data [10–15]. Also, possible strong scattering properties of solvents can make spectral data interpretation very difficult and statistical methods are often necessary.

In this paper we report on *in-line* monitoring of a chemical reaction of the drug entacapone formation by Raman spectroscopy. Entacapone (1), 2-cyano-*N*,*N*-diethyl-3-(3,4-dihydroxy-

* Corresponding author. Tel.: +385 1 4606184; fax: +385 1 4606181.
E-mail address: pnovak@chem.pmf.hr (P. Novak).

0731-7085/$ – see front matter © 2010 Elsevier B.V. All rights reserved.
doi:10.1016/j.jpba.2010.10.012

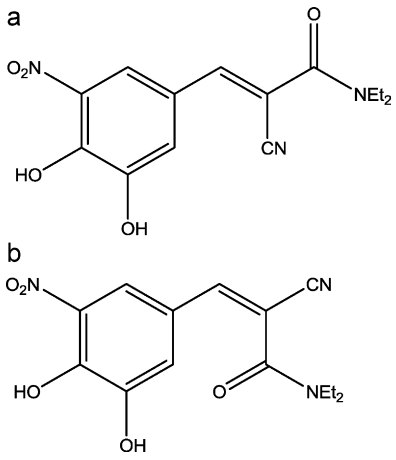

Scheme 1. Structures of (a) *E*- and (b) *Z*-isomer of entacapone.

5-nitrophenyl) propenamide, is a selective inhibitor of catechol-*O*-methyltransferase, an enzyme responsible for the metabolism of L-dopa being a precursor to dopamine. The lack of dopamine is connected to Parkinson's disease. Entacapone is clinically used and prescribed for the treatment of Parkinson's disease [16,17].

Raman spectroscopy has the advantage that it can easily be used for the remote detection through fiber optics facilitating the *in-line* monitoring of chemical reactions and crystallization processes thus generating data in real time. Hence a combination of *in-line* Raman spectroscopy and multivariate analysis [6,17–19] was used to monitor Knoevenagel condensation reaction which is the final step in preparation of entacapone. The reaction gave two isomers of entacapone *E* and *Z* (Scheme 1) in the relative ratio of 2:1 [16]. It was also reported that *E*-isomer was slowly converted to *Z* in human plasma *in vitro* until the ratio 2:1 was reached [20]. We were particularly interested to see whether a combination of Raman spectroscopy and chemometrics could be used to determine entacapone and the reaction end point in the reaction mixture. For comparison the reaction was monitored by the *off-line* Raman spectroscopy and liquid chromatography.

2. Materials and methods

2.1. Materials

3,4-Dihydroxy-5-nitrobenzaldehyde (DHNBA), 2-cyano-*N*,*N*-diethylacetamide (CDEAA) and isobutyl acetate were obtained from

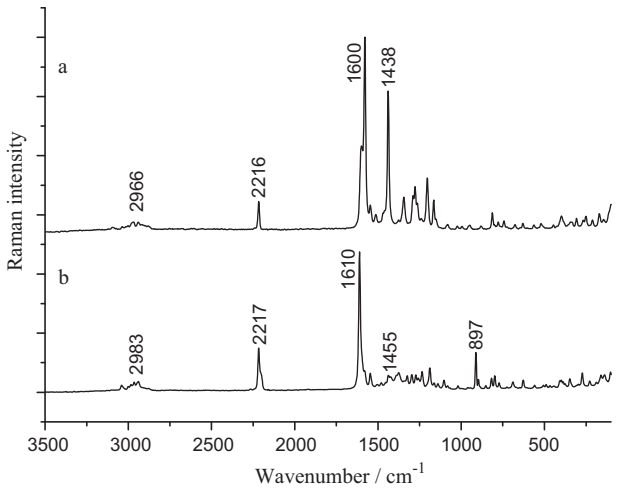

Fig. 1. Raman spectra of (a) *E*- and (b) *Z*-isomer of entacapone.

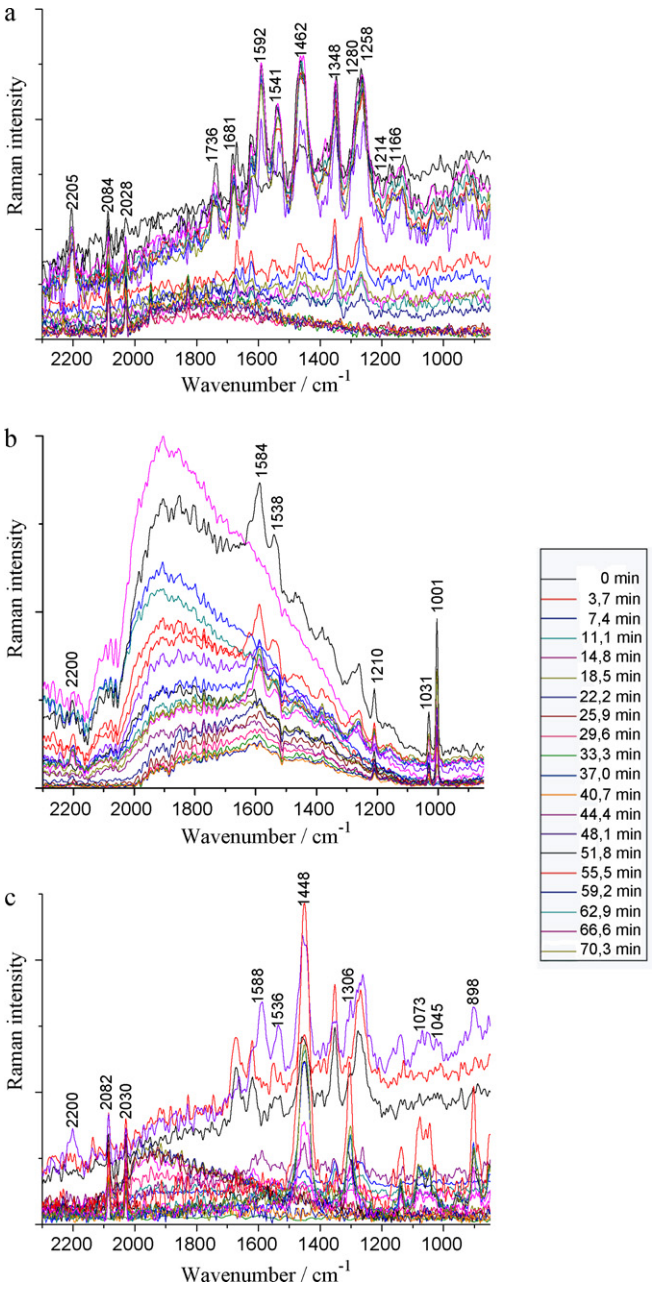

Fig. 2. *In-line* Raman spectra of the Knoevenagel condensation reaction in (a) isobutyl acetate, (b) toluene, and (c) heptane.

PLIVA (Zagreb, Croatia). Methanol (min. 99.5%), heptane (min. 99.8%) and hydrochloric acid (36.5%) were purchased from Kemika (Zagreb, Croatia). Acetic acid (min. 99.8%), piperidine (min. 99%) and toluene (min. 99.5%) were purchased from E. Merck (Darmstadt, Germany), Acros Organics (NJ, USA), Carlo Erba Reagents SpA (Rodano, Italy) and J.T. Baker (Deventer, Holland), respectively.

2.2. Sample preparation

2-Cyano-*N*,*N*-diethyl-3-(3,4-dihydroxy-5-nitrophenyl)propenamide (entacapone) was prepared by the Knoevenagel condensation of 3,4-dihydroxy-5-nitrobenzaldehyde (DHNBA) and 2-cyano-*N*,*N*-diethylacetamide (CDEAA) [1].

Prior to condensation reaction a catalyst, e.g. piperidine acetate was prepared. In a solution of toluene (41 ml) and acetic acid (1.03 ml), piperidine (1.78 ml) was

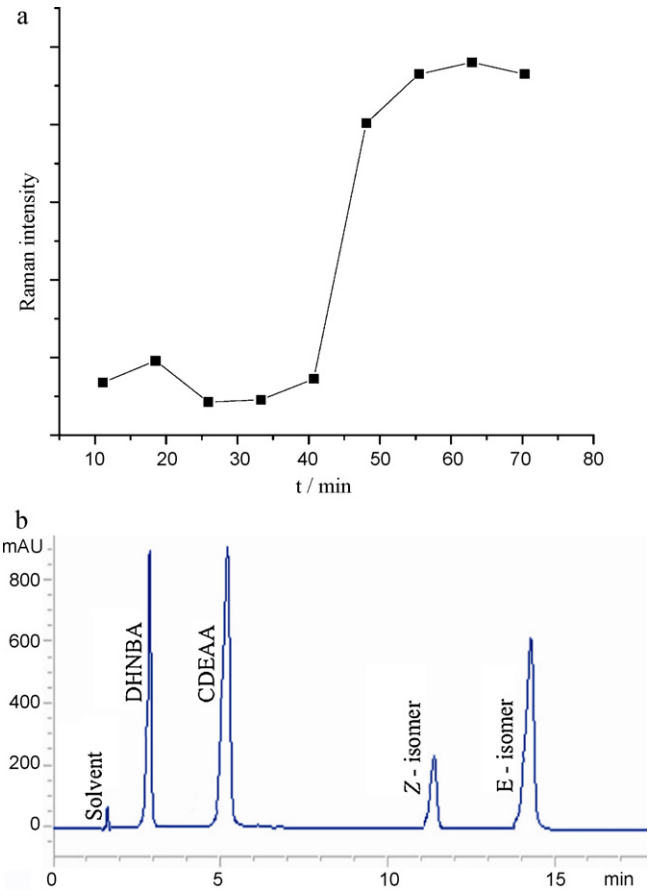

Fig. 3. (a) A representative Raman band intensity of the peak at 1592 cm^{-1} *vs.* reaction time in isobutyl acetate and (b) *off-line* chromatogram of the aliquot taken 40 min after the beginning of the chemical reaction.

added dropwise for 5 min and stirred at room temperature.

After the catalyst was formed, in the reaction mixture were added 3,4-dihydroxy-5-nitrobenzaldehyde (3.0 g), 2-cyano-*N*,*N*-diethylacetamide (2.4 g) and toluene (10 ml). The reaction mixture was heated at 120 °C and stirred under reflux for 1 h. After the separation of approximately 3.2 g of water on Dean-Stark adapter, methanol (7.5 ml) and hydrochloric acid (36.5% w/w, 3.2 ml) were added to dissolve the oily product. The crude product was filtered through a Büchner funnel and washed over with cold toluene (2.3 ml).

The reaction was repeated with heptane and isobutyl acetate as solvents.

2.3. Liquid chromatography

A HP 1090 HPLC system (Hewlett-Packard Company, Palo Alto, CA, USA) comprising a binary pump, autosampler and diode array detector (DAD) set at 210 nm was used with a Phenomenex Gemini column (250 mm × 4.6 mm; 5 μm) and 25 mM aqueous KH_2PO_4:CH_3OH 70:30 v/v as the mobile phase at a flow rate of 1.8 ml/min.

2.4. Raman spectroscopy

FT-Raman spectra were recorded using a Bruker Equinox 55 interferometer equipped with a FRA 160/S Raman module. NIR excitation at 1064 nm was provided by Nd-YAG laser. The laser power was 500 mW. 128 scans were accumulated for each spectrum at a spectral resolution of 4 cm^{-1} in the range between 3500 and 100 cm^{-1}.

2.4.1. Off-line Raman spectroscopy

Samples were taken out of a reaction vessel and measured every 10 min during the chemical reaction. Due to inhomogeneity of the reaction mixture, Raman spectra were recorded separately for the oily residues and solution aliquots. Raman spectra of the filtered crystals of the final products were also recorded.

2.4.2. In-line Raman spectroscopy

The *in-line* spectral data were acquired using the Raman fiber optic immersion probe (optical fibers of 5 m length). The probe was inserted directly into the reaction vessel and Raman spectra were recorded continuously during the chemical reaction (3.7 min per spectrum). After the reaction was completed, Raman spectra of the lower layer (oily product) and upper layer (solvent) were recorded separately and compared to those obtained *in-line*. *In-line* measurements were performed at several levels in the reaction vessel.

Table 1
Characteristic experimental and calculated vibrational frequencies of *E*- and *Z*-isomers of entacapone.

Vibrational mode	$\tilde{\nu}$/cm (IR)[a]		$\tilde{\nu}$/cm (Raman)[a]		$\tilde{\nu}$/cm (calculated)	
	E	*Z*	*E*	*Z*	*E*	*Z*
ν (O–H)	3340	3200–2700			3833, 3747	3845, 3762
ν (C≡N)	2217	2217	2216	2217	2298	2307
ν $(C{=}O)_{amide}$	1606	1622	1600	1610	1700	1702
ν (NO_2)	1544	1549	1545	1546	1598	1599
ν $(C{=}C)_{aromatic}$	1440	1444	1438	1455	1471	1472

[a] Experimental values.

Table 2
Total variance represented in principal components of *in-line* Raman spectra of Knoevenagel condensation reaction in different solvents.

	Total variance (%)					
	Isobutyl acetate		Heptane		Toluene	
	Individual	Cumulative	Individual	Cumulative	Individual	Cumulative
PC1	80.92	80.92	67.92	67.92	99.24	99.24
PC2	14.11	95.03	17.96	85.88	0.52	99.76
PC3	3.27	98.31	13.82	99.70	0.14	99.90

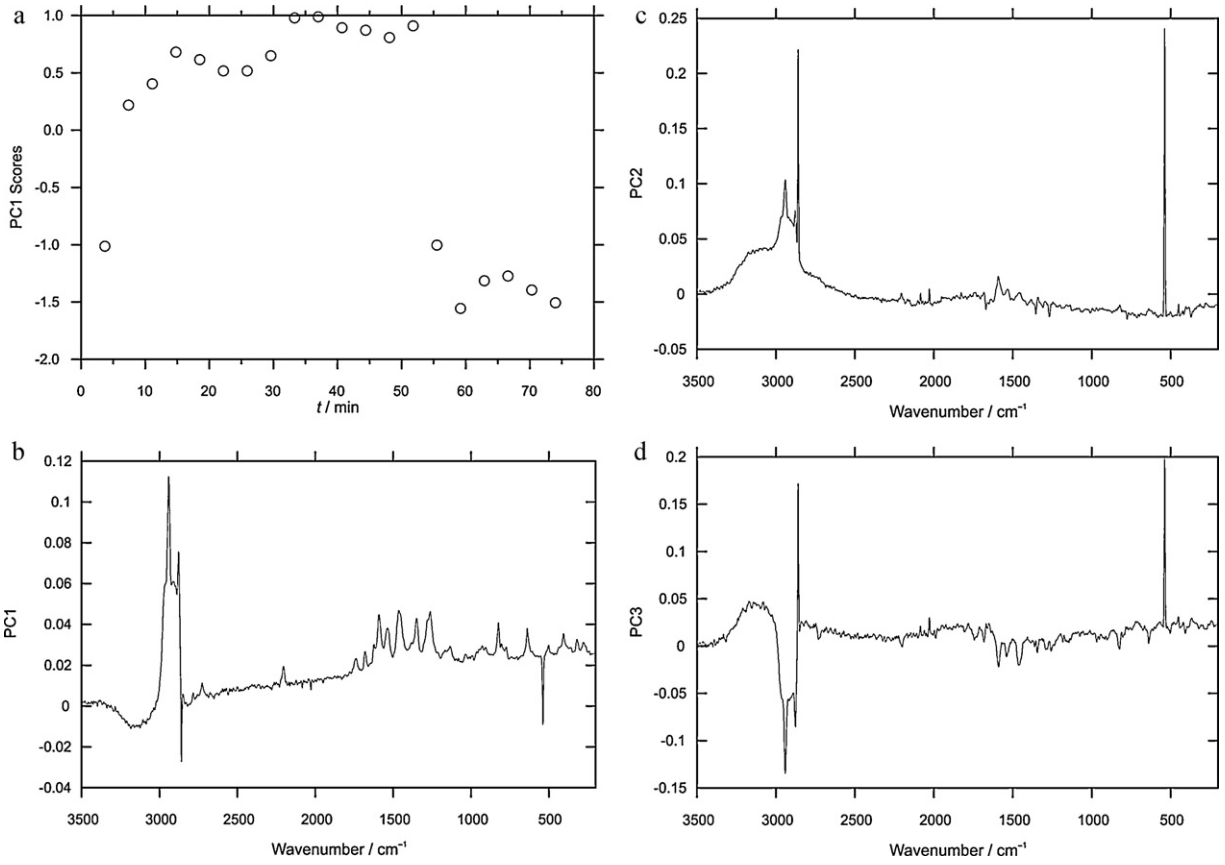

Fig. 4. (a) PC1 scores, (b) PC1, (c) PC2 and (d) PC3 loadings for a set of 20 *in-line* FT-Raman spectra of the chemical reaction in isobutyl acetate.

2.5. Multivariate data analysis

Data obtained by *in-line* FT-Raman spectral measurements of the chemical reaction were exported to the ASCII format and arranged in the matrix (numbers written in a free format). A subset of spectral data in the range (3500–200) cm^{-1} was selected providing a data matrix (dimension n samples × 1712 wavenumbers). Data were mean-centered and PCA of covariance matrix was carried out using our own FORTRAN code (written by TH) based on the NIPALS algorithm suitable for numerical calculation [21]. Most of the calculated eigenvectors converged within 200 iterations.

2.6. DFT calculations

Equilibrium geometries of *E*- and *Z*-isomers of entacapone were calculated using the B3LYP density functional method [22–24] and 6-311++G(3df,3pd) basis set. All calculations were performed using GAUSSIAN 03 package [25]. After geometry optimization, harmonic vibrational frequencies were computed using the same level of theory.

3. Results and discussion

3.1. Knoevenagel condensation reaction

The reaction of 3,4-dihydroxy-5-nitrobenzaldehyde and 2-cyano-*N*,*N*-diethylacetamide gave two isomers of entacapone, *E* and *Z* (Scheme 1). Prior to the reaction a catalyst piperidine acetate was formed which was a prerequisite for the reaction to take place. The reaction mixture was treated with hydrochloric acid and filtrated to separate entacapone isomers. Both isomers are biologically relevant however it is easier to crystallize the *E*-form and to separate it from the reaction mixture. We have used different solvents, e.g. isobutyl acetate, toluene and heptane to obtain higher yields and higher *E*/*Z* ratio. The solvents were also chosen according to their vibrational spectra characteristics, e.g. to avoid severe band overlapping which can make spectral analysis more complicated.

3.2. Off-line Raman spectra

Prior to *in-line* monitoring of chemical reaction *off-line* IR and Raman spectra of the solid substances of the two isomers *E* and *Z* were recorded and their characteristic vibrations were assigned and are given in Table 1. Vibrational frequencies have also been calculated by DFT calculations and compared to those observed experimentally (Table 1). The Raman spectra are displayed in Fig. 1.

In Raman spectra the bands around 3000 cm^{-1} attributed to the CH stretching are weak and therefore less useful for the reaction monitoring. The bands at 2216 and 2217 cm^{-1} are assigned to the C≡N stretching mode for *E*- and *Z*-isomer, respectively. Raman spectra of the two isomers differ in the spectral region 1610–1400 cm^{-1} where stretching vibrations characteristic of C=O, C=C and NO_2 groups occur (Table 1). The prominent feature in the Raman spectrum of *E*-isomer is the vibrational band at 1438 cm^{-1} which is assigned to a combination of aromatic C=C stretching modes. This band was shifted to 1455 cm^{-1} in the Raman spectrum of *Z*-isomer. On the other hand medium intensity band at 897 cm^{-1} was observed for isomer *Z* which was not present in the spectrum of isomer *E* (Fig. 1). Amide C=O stretching vibrations were observed at 1600 and 1610 cm^{-1} for *E*- and *Z*-isomers, respectively. Some of these bands might further be used to follow the progress of the reaction and to differentiate between the two isomeric forms.

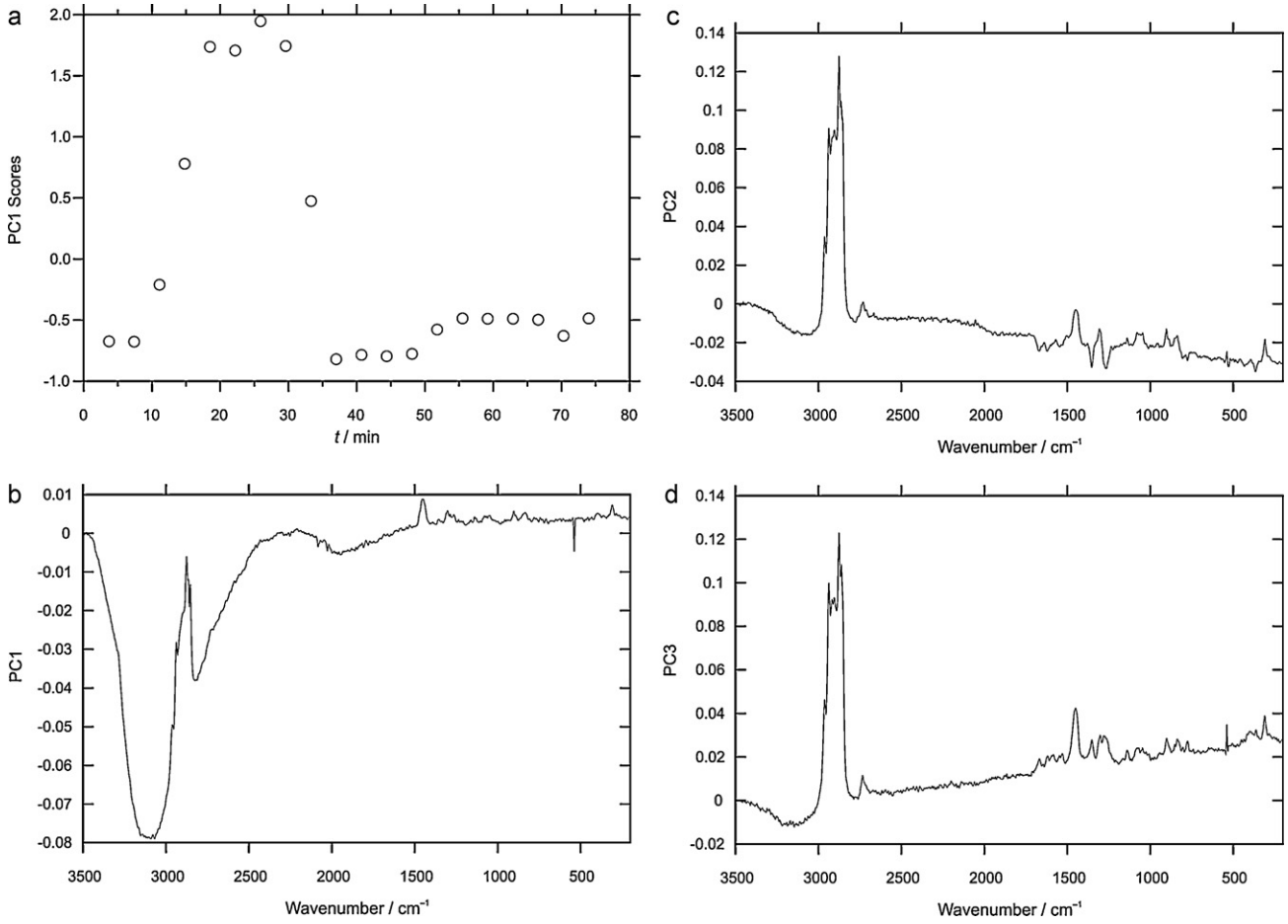

Fig. 5. (a) PC1 scores, (b) PC1, (c) PC2 and (d) PC3 loadings for a set of 20 *in-line* FT-Raman spectra of the chemical reaction in heptane.

3.3. In-line reaction monitoring

The Raman spectra were collected continuously (3.7 min per spectrum) during the chemical reaction by using the Raman probe immersed into the reaction mixture. We performed the measurements at different levels in the vessel to obtain the most intense Raman signals. The *in-line* Raman spectra of the reaction in isobutyl acetate, toluene and heptane are displayed in Fig. 2.

During the course of the reaction in isobutyl acetate, toluene and heptane new bands appeared in the Raman spectra pointing forward to formation of entacapone (Fig. 2). The appearance of a band at ~2200 cm^{-1} can be attributed to C≡N stretching vibration characteristic for both isomers of entacapone. Furthermore, the Raman band observed around 1590 cm^{-1} whose intensity increases as the reaction progresses could be attributed to the amide C=O stretching vibration characteristic of *E*-isomer, as shown in Fig. 3a for the reaction in isobutyl acetate. This band was shifted to lower wavenumbers in comparison with that observed in the solid state (Fig. 1). The *off-line* HPLC analysis of the aliquot taken 40 min after the beginning of the reaction is in agreement with *in-line* results (Fig. 3b). It is clearly seen that both *E*- and *Z*-isomers were formed.

Owing to complexity of the reaction mixtures and severe band overlapping, it was not possible to unambiguously assign other Raman bands and to confirm the formation of *Z*-isomer simply from the *in-line* spectra analysis. Hence, we applied statistics to analyze the measured spectra and to determine the duration of the chemical reaction in each solvent.

3.4. Principal component analysis

Total variances described by principal components of *in-line* FT-Raman spectra are presented In Table 2. For all solvents used the first principal component (PC1) described the greatest extent of variance thus giving a satisfactory description of original data which were confirmed visually.

In the score plots (Figs. 4–6) it can be seen how the reaction proceeds and it is possible to estimate the reaction time. In isobutyl acetate the reaction ended approximately after 50 min. Similarly, the reaction in toluene finished in 46 min with some unexpected reaction profile afterwards. Further investigation is necessary to resolve this issue and to provide additional insights into the reaction mechanism. In the case of heptane, the reaction was the fastest and it ended after 30 min most probably due to lower loss of the catalyst, e.g. piperidine acetate in Dean-Stark adapter. Namely, piperidine acetate has relatively high vapour pressure and some losses occurred in Dean-Stark adapter during the chemical reactions performed at higher temperatures in toluene and isobutyl acetate making a reaction slower. Thus, heptane is the solvent in which the reaction proceeds with the highest rate.

The loading plot in Fig. 4b shows the spectral features responsible for the pattern in the score plot (Fig. 4a). The positive peak in the loading spectrum at 2205 cm^{-1} corresponds to C≡N stretching band present in the Raman spectra of both isomers of entacapone. The presence of this band confirmed that entacapone was formed. Additional bands at 1592, 1214 and 1166 cm^{-1} provided further

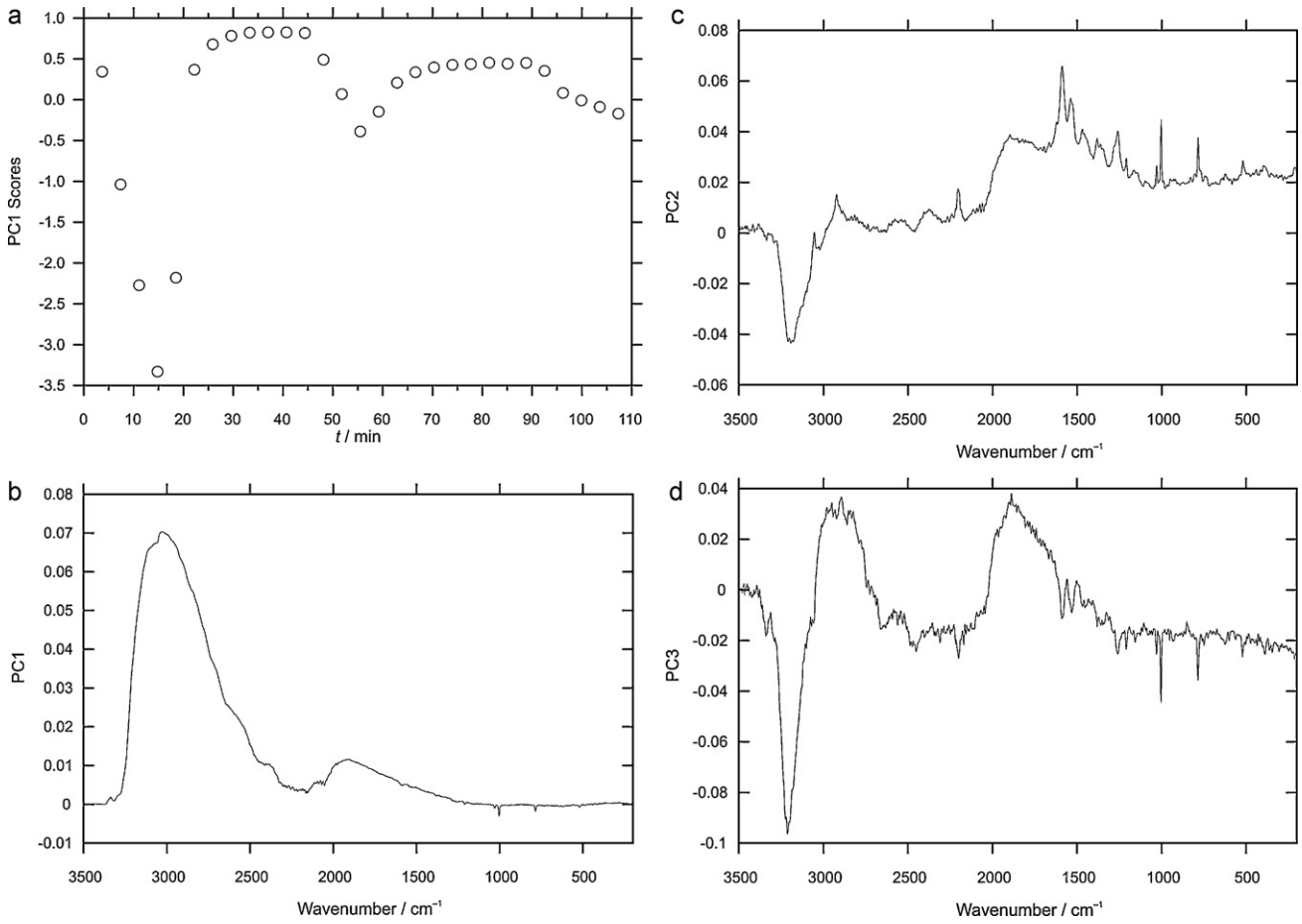

Fig. 6. (a) PC1 scores, (b) PC1, (c) PC2 and (d) PC3 loadings for a set of 29 *in-line* FT-Raman spectra of the chemical reaction in toluene.

evidence of entacapone formation. Bands around 1450 cm^{-1} and 897 cm^{-1} which would confirm the presence of *Z*-isomer are overlapped by the isobutyl acetate bands and in the loading plots can be seen as a shoulder. Hence they can serve only as an indication of *Z*-isomer formation.

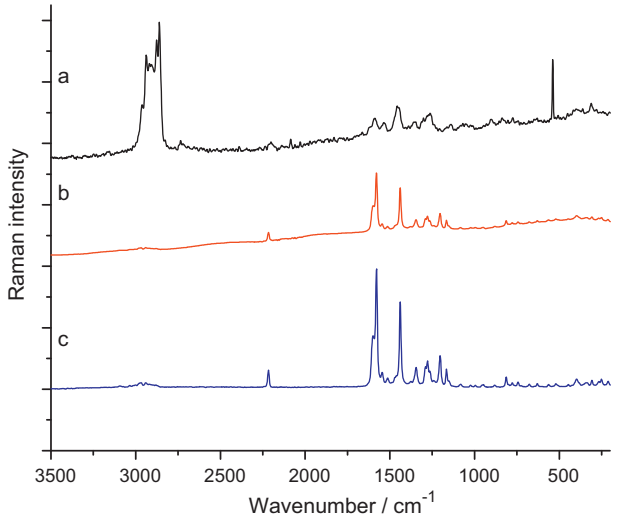

Fig. 7. (a) *In-line* Raman spectrum of entacapone during the synthesis in heptane, (b) *off-line* Raman spectrum of entacapone synthesized in heptane, (c) *off-line* Raman spectrum of pure form A of *E*-isomer of entacapone.

Similar considerations can be applied to reactions in other solvents. Hence, in the loading plots in Figs. 5 and 6b, C≡N stretching band can be unambiguously observed providing a clear evidence of entacapone formation in heptane and toluene.

3.5. Off-line monitoring

3.5.1. Off-line Raman measurements

After the chemical reaction was finished the reaction mixture was treated with hydrochloric acid and filtrated to separate the products of the reaction. The Raman spectra were then recorded and their analysis confirmed that both isomers were formed in the chemical reaction in all solvents. According to Raman spectra analysis of the crystalline *E*-isomer the predominant form in all solvents was found to be the polymorph A [17] as seen in Fig. 7.

3.5.2. HPLC analysis

In order to compare results obtained from *in-line* Raman measurements we have independently monitored chemical reaction by the *off-line* liquid chromatography. During the reaction 1 ml reaction aliquots were sent to HPLC every 10 min. It was shown that both isomers of entacapone *E* and *Z* were formed in Knoevenagel condensation in toluene, heptane and isobutyl acetate (Fig. 3b). From the integrated area peaks the *E*/*Z* relative ratio has been estimated to 2/1, 2.2/1 and 2.3/1 in toluene, heptane and isobutyl acetate, respectively.

4. Conclusion

The Knoevenagel condensation reaction which is the final step in preparation of drug entacapone has been probed by using *in-line* Raman spectroscopy in combination with principal component analysis. It has been shown that PCA of the recorded Raman spectra enables fast end point determination of the chemical reaction in different solvents and identification of entacapone formation. This study demonstrates that Raman spectroscopy and chemometrics can be used for fast and non destructive real time monitoring of entacapone formation reaction and thus have a potential for in-process control.

Acknowledgements

The authors are acknowledged to Ana Kwokal for her helpful comments and suggestions and Ratko Luketa for performing HPLC measurements. This work has been financially supported by The National Foundation for Science, Higher Education and Technological Development of the Republic of Croatia.

Appendix A. Supplementary data

Supplementary data associated with this article can be found, in the online version, at doi:10.1016/j.jpba.2010.10.012.

References

[1] L.X. Yu, R.A. Lionberger, A.S. Raw, R. D'Costa, H. Wu, A.S. Hussain, Applications of process analytical technology to crystallization processes, Adv. Drug Deliv. Rev. 56 (2004) 349–369.
[2] G. Fevotte, In situ Raman spectroscopy for in-line control of pharmaceutical crystallization and solids elaboration processes, Chem. Eng. Res. Des. 85 (2007) 906–920.
[3] J. Cornel, C. Lindenberg, M. Mazzotti, Quantitative application of in situ ATR-FTIR and Raman spectroscopy in crystallization processes, Ind. Eng. Chem. Res. 47 (2008) 4870–4882.
[4] W.P. Findlay, D.E. Bugay, Utilization of Fourier transform-Raman spectroscopy for the study of pharmaceutical crystal forms, J. Pharm. Biomed. Anal. 16 (1998) 921–930.
[5] L.E. O'Brien, P. Timmins, A.C. Williams, P. York, Use of in situ FT-Raman spectroscopy to study the kinetics of the transformation of carbamazepine polymorphs, J. Pharm. Biomed. Anal. 36 (2004) 335–340.
[6] L. Nørgaard, M.H. Hahn, L.B. Knudsen, I.A. Farhat, S.B. Engelsen, Multivariate near–infrared and Raman spectroscopic quantifications of the crystallinity of lactose in whey permeate powder, Int. Dairy J. 15 (2005) 1261–1270.
[7] Y. Hu, J.K. Liang, A.S. Myerson, L.S. Taylor, Crystallization monitoring by Raman spectroscopy: simultaneous measurement of desupersaturation profile and polymorphic form in flufenamic acid systems, Ind. Eng. Chem. Res. 44 (2005) 1233–1240.
[8] G. Fevotte, New perspectives for the on-line monitoring of pharmaceutical crystallization processes using in situ infrared spectroscopy, Int. J. Pharm. 241 (2002) 263–278.
[9] T.R.M. De Beer, W.R.G. Baeyens, J. Ouyang, C. Vervaet, J.P. Remon, Raman spectroscopy as a process analytical technology tool for the understanding and the quantitative in-line monitoring of the homogenization process of a pharmaceutical suspension, Analyst 131 (2006) 1137–1144.
[10] B.J. Kip, T. Berghmans, P. Palmen, A. Van Der Pol, M. Huys, H. Hartwig, M. Scheepers, D. Wienke, On the use of recent developments in vibrational spectroscopic instrumentation in an industrial environment: quicker, smaller and more robust, Vib. Spectrosc. 24 (2000) 75–92.
[11] C.A. McGill, A. Nordon, D. Littlejohn, Comparison of in-line NIR, Raman and UV–visible spectrometries, and at-line NMR spectrometry for the monitoring of an esterification reaction, Analyst 127 (2002) 287–292.
[12] J.R Schmink, J.L. Holcomb, N.E. Leadbeater, Use of Raman spectroscopy as an in situ tool to obtain kinetic data for organic transformations, Chem. Eur. J. 14 (2008) 9943–9950.
[13] V. Calvino Casilda, E. Pérez-Mayoral, M.A. Bañares, E. Lozano Diz, Real-time Raman monitoring of dry media heterogeneous alkylation of imidazole with acidic and basic catalysts, Chem. Eng. J. 161 (2010) 371–376.
[14] S. Li, Application of online reaction monitoring by Raman and infrared spectroscopy in early drug development: halogen–lithium exchange chemistry, Am. Pharm. Rev. 13 (2010) 62–67.
[15] V. Calvino-Casilda, M.A. Banaresa, E. Lozano Diz, Real-time Raman monitoring during coumarins synthesis via Pechmann condensation: a tool for controlling the preparation of pharmaceuticals, Catal. Today (2010), doi:10.1016/j.cattod.2010.01.068.
[16] J. Leppänen, E. Wegelius, T. Nevelainen, T. Järvinen, J. Gynther, J. Huuskonen, Structural studies of acyl esters of entacapone, J. Mol. Struct. 562 (2001) 129–135.
[17] A. Kwokal, T.T.H. Nguyen, K.J. Roberts, Polymorph-directing seeding of entacapone crystallization in aqueous/acetone solution using a self-assembled molecular layer on Au (1 0 0), Cryst. Growth Des. 9 (2009) 4324–4334.
[18] N.N. Daéid, R.J.H. Waddell, The analytical and chemometric procedures used to profile illicit drug seizures, Talanta 67 (2005) 280–285.
[19] N. Failloux, I. Bonnet, M. Baron, E. Perrier, Quantitative analysis of vitamin A degradation by Raman spectroscopy, Appl. Spectrosc. 57 (2003) 1117–1122.
[20] T. Wikberg, P. Ottoila, J. Taskinen, Identification of major urinary metabolites of the catechol-O-methyltransferase inhibitor entacapone in the dog, Eur. J. Drug Metab. Pharmacokinet. 18 (1993) 359–367.
[21] P. Geladi, B. Kowalski, Partial least-squares regression, Anal. Chim. Acta 185 (1986) 1–17.
[22] A.D. Becke, Density-functional thermochemistry. III. The role of exact exchange, J. Chem. Phys. 98 (1993) 5648–5652.
[23] C. Lee, W. Yang, R.G. Parr, Development of the Colle-Salvetti correlation-energy formula into a functional of the electron density, Phys. Rev. B 37 (1988) 785–789.
[24] B. Miehlich, A. Savin, H. Stoll, H. Preuss, Results obtained with the correlation energy density functionals of Becke and Lee, Yang and Parr, Chem. Phys. Lett. 157 (1989) 200–206.
[25] M.J. Frisch, G.W. Trucks, H.B. Schlegel, G.E. Scuseria, M.A. Robb, J.R. Cheeseman, J.A. Montgomery Jr., T. Vreven, K.N. Kudin, J.C. Burant, J.M. Millam, S.S. Iyengar, J. Tomasi, V. Barone, B. Mennucci, M. Cossi, G. Scalmani, N. Rega, G.A. Petersson, H. Nakatsuji, M. Hada, M. Ehara, K. Toyota, R. Fukuda, J. Hasegawa, M. Ishida, T. Nakajima, Y. Honda, O. Kitao, H. Nakai, M. Klene, X. Li, J.E. Knox, H.P. Hratchian, J.B. Cross, V. Bakken, C. Adamo, J. Jaramillo, R. Gomperts, R.E. Stratmann, O. Yazyev, A.J. Austin, R. Cammi, C. Pomelli, J.W. Ochterski, P.Y. Ayala, K. Morokuma, G.A. Voth, P. Salvador, J.J. Dannenberg, V.G. Zakrzewski, S. Dapprich, A.D. Daniels, M.C. Strain, O. Farkas, D.K. Malick, A.D. Rabuck, K. Raghavachari, J.B. Foresman, J.V. Ortiz, Q. Cui, A.G. Baboul, S. Clifford, J. Cioslowski, B.B. Stefanov, G. Liu, A. Liashenko, P. Piskorz, I. Komaromi, R.L. Martin, D.J. Fox, T. Keith, M.A. Al-Laham, C.Y. Peng, A. Nanayakkara, M. Challacombe, P.M.W. Gill, B. Johnson, W. Chen, M.W. Wong, C. Gonzalez, J.A. Pople, Gaussian 03, Revision D.02, Gaussian, Inc., Wallingford, CT, 2004.